Reduced-order modeling for unsteady transonic flows around an airfoil

Rémi Bourguet[a] and Marianna Braza
Institut de Mécanique des Fluides de Toulouse, Allée du Professeur C. Soula, 31400 Toulouse, France

Alain Dervieux
Institut National de Recherche en Informatique et en Automatique, 2004 Route des Lucioles, BP 93, 06902 Sophia-Antipolis, France

High-transonic unsteady flows around an airfoil at zero angle of incidence and moderate Reynolds numbers are characterized by an unsteadiness induced by the von Kármán instability and buffet phenomenon interaction. These flows are investigated by means of low-dimensional modeling approaches. Reduced-order dynamical systems based on proper orthogonal decomposition are derived from a Galerkin projection of two-dimensional compressible Navier-Stokes equations. A specific formulation concerning density and pressure is considered. Reduced-order modeling accurately predicts unsteady transonic phenomena.
[DOI: 10.1063/1.2800042]

A proper orthogonal decomposition (POD) Galerkin method is proposed for reduced-order models (ROMs) of unsteady, high-transonic flows. The specific contribution of this study concerns the development of ROMs issued from the fully compressible time-dependent Navier-Stokes system and their application for the prediction of transonic unsteady flow features. The two-dimensional (2D) transonic flow around a NACA0012 airfoil at zero angle of incidence and moderate chord-based Reynolds number ($\mathrm{Re} \in [0.5, 1] \times 10^4$) represents a challenging configuration to investigate due to the development of an unsteadiness triggered by compressibility effects.[1] At incompressible regimes (Mach number <0.3), this flow is steady. As Mach number (Ma) increases, an instability mode and unsteady phenomena emerge, leading to transition to turbulence. At Mach number 0.3, an undulation appears in the wake. The amplification of this phenomenon as the Mach number increases is responsible for the onset of the von Kármán instability. In the Mach number interval $[0.5, 0.7]$, this mode becomes more pronounced and a periodic alternating vortex pattern is clearly developed. This phenomenon is induced by boundary layer separation downstream of supersonic regions. At Mach number 0.75, a lower frequency phenomenon that corresponds to the oscillation of supersonic pockets on each side of the airfoil is observed. This unsteadiness is the onset of the buffet phenomenon. It is characterized by a strong oscillation of the shock waves at higher Reynolds numbers.[2,3] Fundamental frequencies of these two phenomena are clearly different at moderate Reynolds numbers.[1] Buffet has disappeared at Mach number 0.85, whereas von Kármán vortex shedding is observed until $\mathrm{Ma}=0.95$. In the present study, flow A ($\mathrm{Ma}=0.80$, $\mathrm{Re}=10^4$) is in the range of existence of both phenomena, as the monitoring of Mach number field and pressure coefficient on the airfoil illustrates (Fig. 1). Flow B ($\mathrm{Ma}=0.85$, $\mathrm{Re}=0.5\times10^4$), which is strictly governed by the von Kármán instability, is considered for comparison purpose.

[a]Electronic mail: bourguet@imft.fr

The model reduction method consists of a Galerkin projection of the Navier-Stokes equations onto a low-dimensional basis determined to reach optimal energy reconstruction. This basis is issued from a POD,[4] also known as Karhunen-Loève expansion[5] of flow variables. Various low-order dynamical models have been derived from the Navier-Stokes system under an incompressibility assumption, in 2D (Refs. 6–8) and in three-dimensional (3D) laminar cases[9,10] on the basis of direct numerical simulation datasets. For compressible flows and especially in high-transonic regimes, the coupling of kinematic and thermodynamic variables induces specific difficulties concerning state formulation and inner product involved in POD. In Ref. 11, a general framework is provided to derive low-order models based on inviscid Euler equations, via the POD-Galerkin approach, among others. Frequency-domain POD has been used to reach model reduction of subsonic and transonic flows on the basis of inviscid-viscous models, at high Reynolds numbers (10^6 and above). At first, these ROMs were based on a linearization of the dynamic perturbation about a nonlinear steady flow. This technique achieved efficient predictions of flows around airfoils and turbomachinery cascades oscillating at small amplitudes,[12–14] as well as in 3D aeroelasticity.[15] Recently, a framework using automatic differentiation has been put forward to extend the previous methodology to nonlinear unsteady flow physics, applicable for large oscillations.[16] This approach is promising for flow control based on forced pitching motion of an airfoil that can be envisaged in a further issue of the present study. An isentropic inner product[17] leads to compressible ROMs that are valid for moderate Mach numbers and cold flows. Investigations of stability properties of POD ROMs have been reported in Ref. 18. In the present study, a specific inner product ensuring POD dimensional consistency in the compressible case is defined. This is utilized to extract the POD basis and to perform a Galerkin projection of a modified state system[19] onto the reduced-order subspace.

Assuming time/space separation, a classical truncated

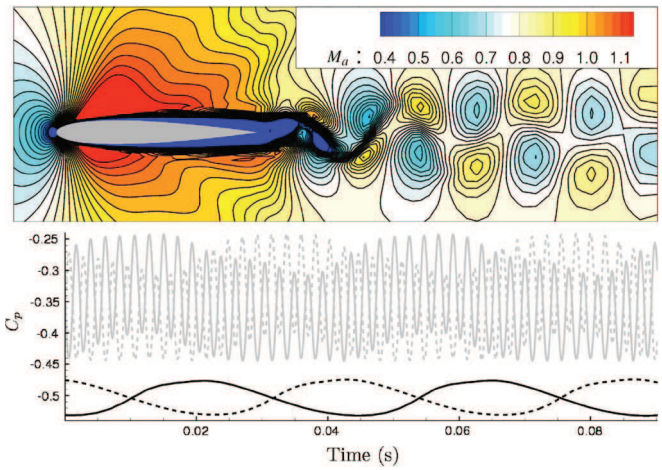

FIG. 1. (Color online) Instantaneous Mach number field and nondimensional pressure coefficient as a function of time, near the leading edge $(x_1/c, x_2/c)=(0.105, \pm 0.047)$ (black) and near the trailing edge $(x_1/c, x_2/c)=(0.92, \pm 0.011)$ (gray) at Ma=0.80 and Re=10^4 (flow A).

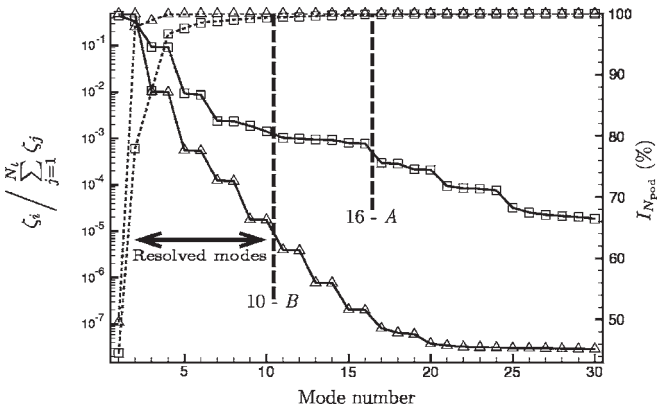

FIG. 2. Normalized eigenvalues (left axis—solid lines) and statistical content of the reduced-order basis (right axis—dashed lines) as a function of mode number in flows A (□) and B (△).

POD expansion yields an approximation of each time/space-dependent quantity $\mathbf{v}$ as a finite linear combination of N_{pod} specific eigenfunctions:

$$\mathbf{v}(\mathbf{x},t)=\sum_{i=1}^{\infty} a_i(t)\mathbf{\Phi}_i(\mathbf{x}) \approx \sum_{i=1}^{N_{\text{pod}}} a_i(t)\mathbf{\Phi}_i(\mathbf{x}), \tag{1}$$

where a_i are time-dependent functions and $\mathbf{\Phi}_i$ orthonormalized stationary spatial modes determined as successive solutions of the following constrained optimization problem:

$$\begin{aligned}&\mathbf{\Phi}_{i+1}=\arg \max_{\mathbf{\Psi}\in L^2(\Omega)^d} \langle (\mathbf{v}-\Pi_i\mathbf{v},\mathbf{\Psi})^2\rangle \\ &\text{subject to} (\mathbf{\Psi},\mathbf{\Psi})=1,\end{aligned} \tag{2}$$

where $\langle\cdot\rangle$ represents time averaging operator, $\Omega\subset\mathbb{R}^2$ is the spatial domain, $(\cdot,\cdot)$ is an inner product that has to be defined on $L^2(\Omega)^d$, and Π_i is the orthogonal projector onto $\mathbf{span}\{\mathbf{\Phi}_1,\ldots,\mathbf{\Phi}_i\}$ for $i\geq 1$, with $\Pi_0\equiv\mathbf{0}_p$. Finding $\mathbf{\Phi}_i$ in Eq. (2) is equivalent to solve a Fredholm integral eigenvalue problem involving a $\mathbf{v}$ two-point space correlation tensor. In the discrete numerical context, the number of space discretization points (N_x) being large in front of the number of "high-order" temporal samples (N_t), "snapshot-POD" technique[20] is used, leading to an eigenproblem on time correlation matrix. In the case of multiple state variables and especially in the compressible case (here, $d=4$), the inner product adopted to extract the POD basis has to be carefully defined.[17] The following weighted spatial product is suggested:

$$(\mathbf{v}^{\text{I}},\mathbf{v}^{\text{II}})=\sum_{i=1}^{d}\int_{\Omega}\frac{v_i^{\text{I}}v_i^{\text{II}}}{\sigma_i^2+\varepsilon}d\mathbf{x}, \tag{3}$$

where $\mathbf{v}^{\text{I}}$ and $\mathbf{v}^{\text{II}}$ are two states involving d variables and $\sigma_i^2(\mathbf{x})=(1/T_s)\int_{t_0}^{t_0+T_s}(v_i(\mathbf{x},t)-\overline{v_i(\mathbf{x})})^2dt$. T_s is the snapshot storage period and $\overline{v_i(\mathbf{x})}=\langle v_i(\mathbf{x},\cdot)\rangle$. σ_i^2 is the local temporal statistical variance of v_i. ε is a small positive constant. This definition ensures POD dimensional consistency and leads to a considerable reduction of the number of degrees of freedom; i.e., from $4\times N_x$ to N_{pod}, with $N_{\text{pod}}\ll N_x$ and $N_{\text{pod}}\ll N_t$. Time evolution of the whole state vector is then described by a single nondimensional dynamic for each POD mode. State variable fluctuations are approximated by

$$v_i(\mathbf{x},t)-\overline{v_i(\mathbf{x})}\approx\sum_{j=1}^{N_{\text{pod}}} a_j(t)\Phi_j^{v_i}(\mathbf{x}). \tag{4}$$

The POD is performed on the fluctuations because spatial POD modes can only respect homogeneous boundary conditions. Two-dimensional Navier-Stokes simulations are issued from ICARE/IMFT compressible finite volume solver, validated for the present test cases with a C-type grid ($N_x=369\times 89$ nodes).[1]

In flow A, the "high-order" dataset contains $N_t=2200$ snapshots collected regularly over one buffet period of the established flow ($\Delta_t=1.9\times10^{-5}$ s), which corresponds approximately to 20 von Kármán periods. $N_t=100$ samples are stored over one period of vortex shedding in flow B ($\Delta_t=2.6\times10^{-5}$ s). After performing POD basis extraction, the mode truncation is founded on the statistical content conveyed by the first N_{pod} modes $I_{N_{\text{pod}}}=\Sigma_{i=1}^{N_{\text{pod}}}\zeta_i/\Sigma_{i=1}^{N_t}\zeta_i$, where ζ_i are time/space two-point correlation matrix eigenvalues. $I_{N_{\text{pod}}}=99.9\%$ is arbitrarily chosen, which induces $N_{\text{pod}}=16$ in flow A, whereas ten modes are sufficient in B (Fig. 2). Flow A involves more complex flow dynamics, which implies a significant increase of the informational content conveyed by the second pair of modes (18.5% versus 2% in flow B).

Direct POD expansion of conservative variables in Navier-Stokes governing equations leads to fractional expressions that do not allow trivial Galerkin projections. However, an alternative is suggested by Ref. 19 to derive quadratic fluxes for compressible Navier-Stokes system by considering a modified formulation of state vector $\mathbf{U}=[\rho,\rho u_1,\rho u_2,\rho e]^t\rightarrow\hat{\mathbf{U}}=[1/\rho,u_1,u_2,p]^t$. ρ is the density and u_i are velocity components. e represents total energy, defined by $e=C_vT+(u_1^2+u_2^2)/2$, where T is the temperature and C_v the specific heat coefficient. p is the thermodynamic pressure, which satisfies the ideal gas law $p=\rho RT$, and R is the ideal gas constant. The corresponding modified state system is projected onto the truncated POD basis, for $i=1,\ldots,N_{\text{pod}}$:

$$(\hat{\mathbf{U}}_{,t} + \mathbf{A}_\alpha \hat{\mathbf{U}}_{,\alpha}, \mathbf{\Phi}_i) = (\mathbf{F}^v_{\alpha,\alpha} - \mathbf{G}^v_\alpha, \mathbf{\Phi}_i). \tag{5}$$

POD expansion is applied to state variables, leading to following approximations:

$$\mathbf{A}_i \approx \sum_{j=1}^{N_{\text{pod}}+1} a_j^\star \begin{bmatrix} \Phi_j^{\star u_i} & -\Phi_j^{\star(1/\rho)}\delta_{1i} & -\Phi_j^{\star(1/\rho)}\delta_{2i} & 0 \\ 0 & \Phi_j^{\star u_i} & 0 & \Phi_j^{\star(1/\rho)}\delta_{1i} \\ 0 & 0 & \Phi_j^{\star u_i} & \Phi_j^{\star(1/\rho)}\delta_{2i} \\ 0 & \gamma\Phi_j^{\star p}\delta_{1i} & \gamma\Phi_j^{\star p}\delta_{2i} & \Phi_j^{\star u_i} \end{bmatrix}, \tag{6}$$

$$\mathbf{F}_i^v \approx \sum_{j,k=1}^{N_{\text{pod}}+1} a_j^\star a_k^\star \begin{bmatrix} 0 \\ \Phi_j^{\star(1/\rho)}[\mu(\Phi_{k,i}^{\star u_1} + \Phi_{k,1}^{\star u_i}) + \lambda\Phi_{k,\alpha}^{\star u_\alpha}\delta_{1i}] \\ \Phi_j^{\star(1/\rho)}[\mu(\Phi_{k,i}^{\star u_2} + \Phi_{k,2}^{\star u_i}) + \lambda\Phi_{k,\alpha}^{\star u_\alpha}\delta_{2i}] \\ \frac{\gamma\mu}{\text{Pr}}[\Phi_j^{\star p}\Phi_{k,i}^{\star(1/\rho)} + \Phi_{j,i}^{\star p}\Phi_k^{\star(1/\rho)}] \end{bmatrix}, \tag{7}$$

$$\mathbf{G}_i^v \approx \sum_{j,k=1}^{N_{\text{pod}}+1} a_j^\star a_k^\star \begin{bmatrix} 0 \\ \Phi_{j,i}^{\star(1/\rho)}[\mu(\Phi_{k,i}^{\star u_1} + \Phi_{k,1}^{\star u_i}) + \lambda\Phi_{k,\alpha}^{\star u_\alpha}\delta_{1i}] \\ \Phi_{j,i}^{\star(1/\rho)}[\mu(\Phi_{k,i}^{\star u_2} + \Phi_{k,2}^{\star u_i}) + \lambda\Phi_{k,\alpha}^{\star u_\alpha}\delta_{2i}] \\ (1-\gamma)\Phi_{j,i}^{\star u_\alpha}[\mu(\Phi_{k,i}^{\star u_\alpha} + \Phi_{k,\alpha}^{\star u_i}) + \lambda\Phi_{k,\beta}^{\star u_\beta}\delta_{\alpha i}] \end{bmatrix}, \tag{8}$$

where $\mathbf{a}^\star = [1, a_1, \ldots, a_{\text{pod}}] = [1, \mathbf{a}]$ and $\mathbf{\Phi}^\star = [\hat{\mathbf{U}}, \mathbf{\Phi}_1, \ldots, \mathbf{\Phi}_{\text{pod}}]$. μ is the fluid viscosity, λ is the Lamé coefficient, γ the polytropic coefficient, Pr the Prandtl number, and δ_{ij} is the Kronecker symbol. $\cdot_{,t}$ and $\cdot_{,i}$ denote, respectively, time and space derivatives. For more clarity, Greek subscripts are used to specify implicit summations and POD expansions are explicit. Only time-independent boundary conditions are prescribed. In particular, no-slip condition and constant temperature are imposed on the airfoil.

The modified state system being quadratic, the Galerkin projection onto the truncated POD basis yields a quadratic polynomial ordinary differential equation system, as in the incompressible case, for $i = 1, \ldots, N_{\text{pod}}$:

$$\begin{aligned} \dot{a}_i &= (C_i + C_i^s) + \sum_{j=1}^{N_{\text{pod}}} (L_{ij} + L_{ij}^s) a_j + \sum_{j,k=1}^{N_{\text{pod}}} Q_{ijk} a_j a_k \\ &= f_i(\mathbf{C}^s, \mathbf{L}^s, \mathbf{a}), \\ a_i(t_0) &= [\hat{\mathbf{U}}(\cdot, t_0) - \overline{\hat{\mathbf{U}}}, \mathbf{\Phi}_i]. \end{aligned} \tag{9}$$

C_i, L_{ij}, and Q_{ijk} are constant coefficients issued from the Galerkin projection of the modified state system (5). Linear and constant terms are involved because of time-averaged value subtraction. As reported in Ref. 21, POD Galerkin ROM is structurally unstable, which leads to dynamic amplitude growth/decrease and phase-lag occurring when performing long time integrations. Many calibration and stabilization methods have been reported in the literature: addition of artificial dissipations,[22] "data-driven" optimizations,[23] addition of "shift modes" in the empirical basis,[21] and more recently, an "intrinsic stabilization" procedure,[24] among others. In the present study, C_i^s and L_{ij}^s coefficients are determined so as to minimize the mean square of prediction error with respect to reference dynamics: $J(\mathbf{C}^s, \mathbf{L}^s) = \frac{1}{2}\sum_{i=1}^{N_{\text{pod}}}\sum_{j=1}^{N_t}\{a_i(t_j) - a_i(t_0) - \int_{t_0}^{t_j} f_i[\mathbf{C}^s, \mathbf{L}^s, \mathbf{a}_{\text{rom}}(t)]dt\}^2$, where $\mathbf{a}_{\text{rom}}$ are predicted dynamics issued from Eq. (9). In a similar way to Ref. 25 in the incompressible case, this optimization problem is turned into a linear system resolution by considering reference dynamics in the Cauchy problem integration. ROM integration is performed with a fourth-order-accurate Runge-Kutta scheme over a snapshot temporal horizon.

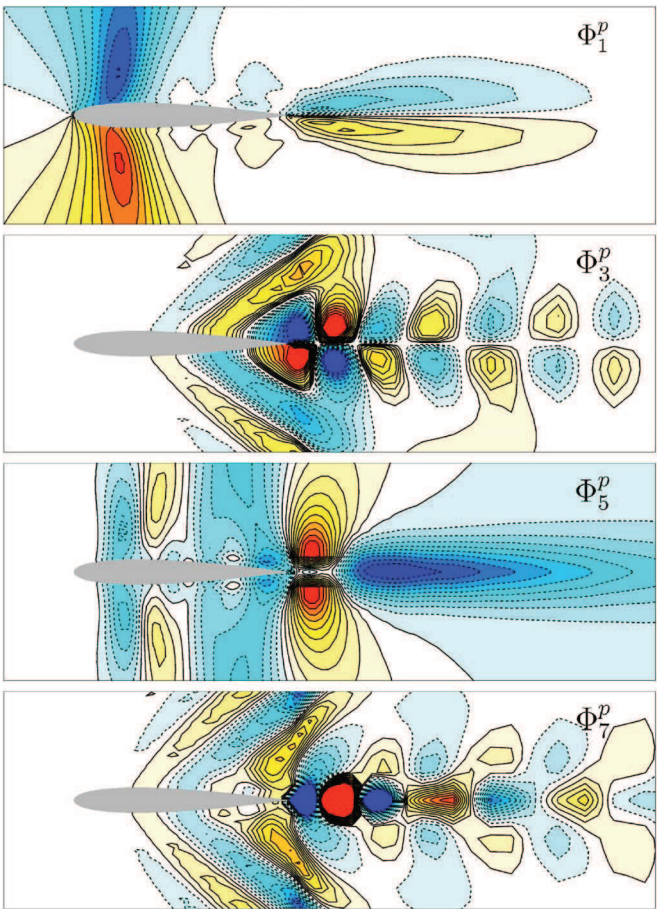

FIG. 3. (Color online) First four odd spatial POD modes associated to pressure in flow A (Ma=0.80, Re=10^4), where the von Kármán instability interacts with the buffet phenomenon. Positive (negative) values are denoted by solid (dashed) lines.

As presented in Fig. 3, POD methodology enables an efficient identification of the main phenomena responsible for flow unsteadiness (flow A). The buffet phenomenon is efficiently described by the two first modes, whereas the following pair is related to the high-frequency von Kármán instability. Moreover, POD modes provide information concerning flow topology and spatial correlations: as can be observed on Φ_1^p, the oscillation of supersonic pockets on each side of the airfoil is clearly correlated with slow pressure fluctuations and flow meandering occurring in the near wake, at buffet frequency. POD mode dynamics also exhibit this physical decoupling. As shown in Fig. 4, a strong interaction between the two phenomena appears on seventh mode. In contrast, each of the first six modes exhibits the

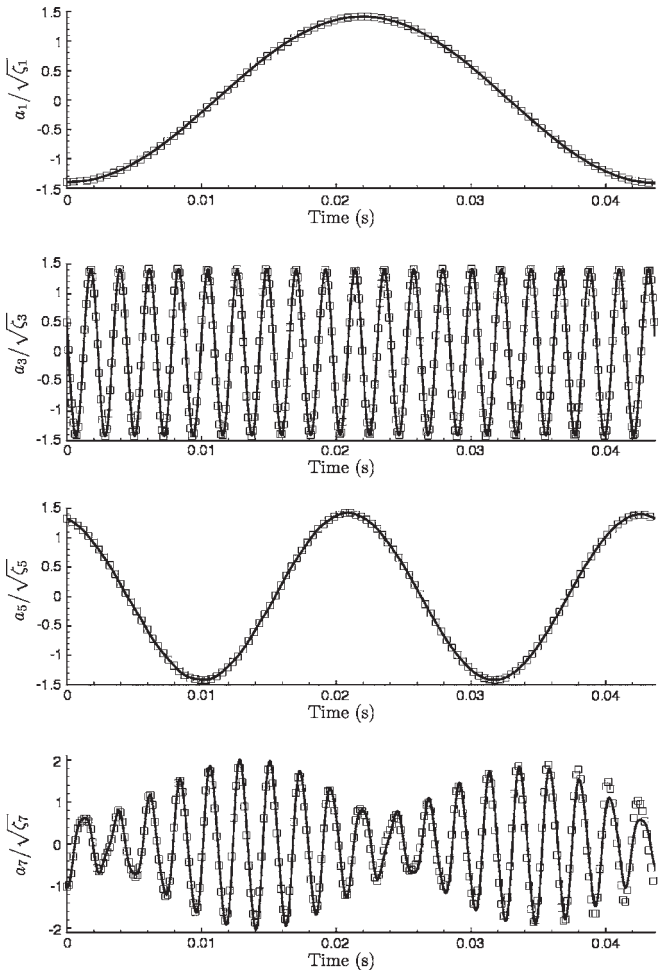

FIG. 4. First four odd normalized POD dynamics (flow A): references issued from high-order database projections (□) and prediction by 16-mode ROM (solid lines).

effect of only one frequency. The dynamics issued from ROM integration present an excellent match with those issued from the Navier-Stokes simulation, even for the last modes (Fig. 4). The relative state variable prediction error based on the consistent inner product [Eq. (3)] is monitored at each time step and remains lower than $(1.5\times10^{-6})\%$ for both flows, which is in the same order of magnitude as POD basis truncation error.

To summarize, a low-dimensional model for *compressible flows* has been derived via POD-Galerkin methodology on the basis of a modified formulation of Navier-Stokes governing equations. The flow physics are governed by two main unsteady phenomena induced by compressibility effects, i.e., von Kármán instability and buffeting, which were well identified by POD analysis. The stabilized ROM achieved faithful unsteadiness predictions in the high-transonic regime.

[1] A. Bouhadji and M. Braza, "Organised modes and shock-vortex interaction in unsteady viscous transonic flows around an aerofoil, Part I: Mach number effect," Comput. Fluids **32**, 1233 (2003).

[2] H. L. Seegmiller, J. G. Marvin, and L. L. Levy, "Steady and unsteady transonic flow," AIAA J. **16**, 1262 (1978).

[3] S. Raghunathan, R. D. Mitchell, and M. A. Gillan, "Transonic shock oscillations on NACA0012 aerofoil," Shock Waves **8**, 191 (1998).

[4] G. Berkooz, P. Holmes, and J. L. Lumley, "The proper orthogonal decomposition in the analysis of turbulent flows," Annu. Rev. Fluid Mech. **25**, 539 (1993).

[5] K. Karhunen, "Zur Spektraltheorie stochasticher Prozesse," Ann. Acad. Sci. Fenn., Ser. A1: Math.-Phys. **A1**, 34 (1946).

[6] A. E. Deane, I. G. Kevrekidis, G. E. Karniadakis, and S. A. Orszag, "Low-dimensional models for complex geometry flows: Application to grooved channels and circular cylinders," Phys. Fluids A **3**, 2337 (1991).

[7] W. Cazemier, R. W. C. P. Verstappen, and A. E. P. Veldman, "Proper orthogonal decomposition and low-dimensional models for driven cavity flows," Phys. Fluids **10**, 1685 (1998).

[8] M. Bergmann, L. Cordier, and J. P. Brancher, "Optimal rotary control of the cylinder wake using POD reduced order model," Phys. Fluids **17**, 097101 (2005).

[9] X. Ma and G. E. Karniadakis, "A low-dimensional model for simulating three-dimensional cylinder flow," J. Fluid Mech. **458**, 181 (2002).

[10] M. Buffoni, S. Camarri, A. Iollo, and M. V. Salvetti, "Low-dimensional modelling of a confined three-dimensional wake flow," J. Fluid Mech. **569**, 141 (2006).

[11] D. J. Lucia and P. S. Beran, "Projection methods for reduced order models of compressible flows," J. Comput. Phys. **188**, 252 (2003).

[12] K. C. Hall, J. P. Thomas, and E. H. Dowell, "Proper orthogonal decomposition technique for transonic aerodynamic flows," AIAA J. **38**, 1853 (2000).

[13] B. I. Epureanu, E. H. Dowell, and K. C. Hall, "Reduced-order models of unsteady transonic viscous flows in turbomachinery," J. Fluids Struct. **14**, 1215 (2000).

[14] B. I. Epureanu, E. H. Dowell, and K. C. Hall, "Reduced-order models of unsteady viscous flows in turbomachinery using viscous-inviscid coupling," J. Fluids Struct. **15**, 255 (2001).

[15] J. P. Thomas, E. H. Dowell, and K. C. Hall, "Three-dimensional transonic aeroelasticity using proper orthogonal decomposition-based reduced-order models," J. Aircr. **40**, 544 (2003).

[16] J. P. Thomas, E. H. Dowell, and K. C. Hall, "Using automatic differentiation to create a nonlinear reduced order model of a computational fluid dynamic solver," AIAA Paper 2006–7115.

[17] C. W. Rowley, T. Colonius, and R. M. Murray, "Model reduction for compressible flows using POD and Galerkin projection," Physica D **189**, 115 (2004).

[18] A. Iollo, S. Lanteri, and J. A. Desideri, "Stability properties of POD-Galerkin approximations for the compressible Navier-Stokes equations," Theor. Comput. Fluid Dyn. **13**, 377 (2000).

[19] G. Vigo, A. Dervieux, M. Mallet, M. Ravachol, and B. Stoufflet, "Extension of methods based on the proper orthogonal decomposition to the simulation of unsteady compressible Navier-Stokes flows," in *Computational Fluid Dynamics'98, Proceedings of the Fourth ECCOMAS Conference* (Wiley, New York, 1998), pp. 648–653.

[20] L. Sirovich, "Turbulence and the dynamics of coherent structures. I–Coherent structures," Q. Appl. Math. **45**, 561 (1987); "Turbulence and the dynamics of coherent structures. II–Symmetries and transformations," Q. Appl. Math. **45**, 573 (1987); "Turbulence and the dynamics of coherent structures. III–Dynamics and scaling," Q. Appl. Math. **45**, 583 (1987).

[21] B. R. Noack, K. Afanasiev, M. Morzynski, G. Tadmor, and F. Thiele, "A hierarchy of low-dimensional models for the transient and post-transient cylinder wake," J. Fluid Mech. **497**, 335 (2003).

[22] S. Sirisup and G. E. Karniadakis, "A spectral viscosity method for correcting the long-term behavior of POD models," J. Comput. Phys. **194**, 92 (2004).

[23] B. Galletti, C. H. Bruneau, L. Zannetti, and A. Iollo, "Low-order modelling of laminar flow regimes past a confined square cylinder," J. Fluid Mech. **503**, 161 (2004).

[24] V. L. Kalb and A. E. Deane, "An intrinsic stabilization scheme for proper orthogonal decomposition based low-dimensional models," Phys. Fluids **19**, 054106 (2007).

[25] M. Couplet, C. Basdevant, and P. Sagaut, "Calibrated reduced-order POD-Galerkin system for fluid flow modelling," J. Comput. Phys. **207**, 192 (2005).